Original Article | Cardiovascular Imaging

http://dx.doi.org/10.3348/kjr.2016.17.3.321
pISSN 1229-6929 · eISSN 2005-8330
Korean J Radiol 2016;17(3):321-329

Korean Journal of Radiology
KJR

Virtual Non-Contrast CT Using Dual-Energy Spectral CT: Feasibility of Coronary Artery Calcium Scoring

Inyoung Song, MD[1], Jeong Geun Yi, MD[1], Jeong Hee Park, MD[1], Sung Mok Kim, MD[2], Kyung Soo Lee, MD[2], Myung Jin Chung, MD[2, 3]

[1]Department of Radiology, Konkuk University School of Medicine, Seoul 05030, Korea; [2]Department of Radiology, Samsung Medical Center, Sungkyunkwan University School of Medicine, Seoul 06351, Korea; [3]Department of Digital Health, SAIHST, Sungkyunkwan University, Seoul 06351, Korea

Objective: To evaluate the feasibility of coronary artery calcium scoring based on three virtual noncontrast-enhanced (VNC) images derived from single-source spectral dual-energy CT (DECT) as compared with true noncontrast-enhanced (TNC) images.
Materials and Methods: This prospective study was conducted with the approval of our Institutional Review Board. Ninety-seven patients underwent noncontrast CT followed by contrast-enhanced chest CT using single-source spectral DECT. Iodine eliminated VNC images were reconstructed using two kinds of 2-material decomposition algorithms (material density iodine-water pair [MDW], material density iodine-calcium pair [MDC]) and a material suppressed algorithm (material suppressed iodine [MSI]). Two readers independently quantified calcium on VNC and TNC images. The Spearman correlation coefficient test and Bland-Altman method were used for statistical analyses.
Results: Coronary artery calcium scores from all three VNC images showed excellent correlation with those from the TNC images (Spearman's correlation coefficient [ρ] = 0.94, 0.88, and 0.89 for MDW, MDC, and MSI, respectively; $p < 0.001$ for all pairs). Measured coronary calcium volumes from VNC images also correlated well with those from TNC images (ρ = 0.92, 0.87, and 0.91 for MDW, MDC, and MSI, respectively; $p < 0.001$ for all pairs). Among the three VNC images, coronary calcium from MDW correlated best with that from TNC. The coronary artery calcium scores and volumes were significantly lower from the VNC images than from the TNC images ($p < 0.001$ for all pairs).
Conclusion: The use of VNC images from contrast-enhanced CT using dual-energy material decomposition/suppression is feasible for coronary calcium scoring. The absolute value from VNC tends to be smaller than that from TNC.
Index terms: *Coronary artery disease; Computed tomography; Dual energy*

INTRODUCTION

The coronary artery calcium score (CACS) based on computed tomography (CT) is recognized as an independent and incremental predictor of cardiovascular events for clinical risk stratification (1-5). Coronary artery calcium (CAC) scoring is usually performed by noncontrast-enhanced electrocardiogram (ECG)-gated CT examination prior to contrast-enhanced coronary CT angiography (CCTA) because of the difficulty in identifying and quantifying calcium in the presence of iodine in contrast media. Although some investigations have reported threshold-based measurements of CAC from contrast-enhanced CCTA (6-9), differentiation between calcification and iodinated contrast may be hampered by their high attenuation on CT.

Dual-energy CT (DECT) scanning refers to simultaneous acquisition of datasets at two different X-ray spectra during a single CT acquisition (10, 11). DECT yields information

Received September 2, 2015; accepted after revision February 3, 2016.
Corresponding author: Myung Jin Chung, MD, Department of Radiology, Samsung Medical Center, Sungkyunkwan University School of Medicine, 81 Irwon-ro, Gangnam-gu, Seoul 06351, Korea.
• Tel: (822) 3410-2519 • Fax: (822) 3410-2559
• E-mail: mjchung@skku.edu

about energy-dependent changes in the attenuation of different materials and provides decomposition images for material characterization (10, 12, 13). Virtual noncontrast-enhanced (VNC) images derived from DECT have the potential to reduce the radiation dose and scan time by obviating the need for true noncontrast-enhanced (TNC) images. Whereas dual-source DECT scanning uses an image-based three-material decomposition algorithm, spectral CT scanning using a single-source and single-detector system with a fast kVp-switching mode uses a projection-based two-material decomposition algorithm (14, 15). This scanning mode can provide various types of material decomposition images using different base material pairs (e.g., water- and calcium-based), such that iodine subtraction from base material pairs can provide various VNC images (16).

To date, a few studies have reported on the possible application of VNC images for quantification of coronary calcium using single-source fast kVp-switching DECT coronary angiography (17, 18). To the best of our knowledge there are no published clinical studies that assess CAC using various VNC images from ungated spectral chest DECT. The aim of this study was to evaluate the feasibility of determining the CACS using three different VNC images derived from single-source spectral DECT as compared with CACS determined from TNC images.

MATERIALS AND METHODS

Patients

This prospective study was conducted with the approval of our Institutional Review Board and all patients gave written informed consent. From January to April 2013, we prospectively enrolled patients who met the following inclusion criteria: age > 20 years old; scheduled for noncontrast-enhanced and contrast-enhanced chest CT on a specific scanner for the evaluation of known or suspected inflammatory/infectious disease or malignancy in the thorax. The exclusion criteria were as follows: age < 20 years old; prior coronary artery bypass grafting; prior percutaneous coronary intervention, prior implantation of pacemaker or internal defibrillator lead; prior prosthetic heart valve implantation; known complex congenital heart disease; serum creatinine level > 1.5 mg/dL; contraindication to iodinated contrast material, such as history of anaphylactoid reaction; pregnancy or unknown pregnancy status in patients of childbearing potential; morbid obesity (body mass index calculated as weight in kilograms divided by the square of the height in meters > 40 kg/mm^2). A total of 97 consecutive patients (60 men, 37 women; mean age, 67.5 ± 7.4 years; range, 50–84 years) were included in this study.

CT Examination

All patients underwent CT examination using a high-definition CT scanner (Discovery CT 750 HD FREEdom Edition, GE Healthcare, Waukesha, WI, USA) with a 64 x 0.625 mm detector collimation and a Z-coverage of 40-mm. All patients underwent single-energy noncontrast-enhanced CT followed by dual-energy contrast-enhanced CT scanning at end inspiration. Scanning was performed from the thoracic inlet to the middle portion of the kidney with the patient in a supine position. The TNC scanning was initially performed in the conventional helical mode with a tube voltage of 120 kVp. Contrast-enhanced scans using the dual-energy spectral CT mode (gemstone spectral imaging [GSI] mode) with a single-tube, fast-kVp switching between 80 kVp and 140 kVp in less than 0.5 msec, were obtained 65 seconds after administration of contrast material (100 mL of iopamidol: iomeron 300; Bracco, Milan, Italy) at a rate of 1.5 mL/sec using a power injector. The scan parameters were as follows: helical mode, detector coverage of 40 mm, section thickness of 2.5 mm, reconstruction interval of 2.5 mm, collimator width of 64 x 0.625 mm, pitch of 1.375, gantry rotation speed of 0.5 seconds, and adaptive mA.

Data Postprocessing and Image Reconstruction

Gemstone spectral imaging data postprocessing was performed using a spectral imaging viewer (GSI Viewer; GE Healthcare), which provides a suite of GSI processing tools for the generation of monochromatic energy image data as well as operator-selectable material basis pairs for material basis image creation and clinical viewing (DICOM compatible). Three different VNC images were created from postprocessing (Fig. 1). Two different types of VNC image using two kinds of 2-material decomposition algorithms were reconstructed from contrast-enhanced spectral CT acquisition for analysis: 1) material density iodine-water pair (MDW) images (water equivalent density image based on the material-decomposition of water and iodine pair) and 2) material density iodine-calcium pair (MDC) images (calcium equivalent density image based on the material-decomposition of calcium and iodine pair). Material suppressed iodine (MSI) images (iodine suppressed image in which the volume fraction of contrast is replaced by the

Korean Journal of Radiology
KJR

exact same volume fraction of blood by using multi-material decomposition) were also reconstructed.

Calcium Quantification of the Coronary Artery and Other Vessels

Total calcium scores and volumes from VNC (MDW, MDC, and MSI) images were measured in a blinded manner with an independent workstation (Advantage workstation 4.4: GE Healthcare). The software package (GSI Viewer: GE Healthcare) automatically calculated and displayed the CT attenuation values for the VNC images. The calcium was evaluated in 4 different vascular beds included within the chest CT scan: coronary arteries, the proximal neck vessels, the aortic arch, and the descending thoracic aorta. The calcium scores and volumes of three vascular beds (the proximal neck vessels, the aortic arch, and the descending thoracic aorta) were summarized and expressed as 'other vessels'. Two board-certified radiologists with 10 years and 7 years of experience performed all measurements by consensus.

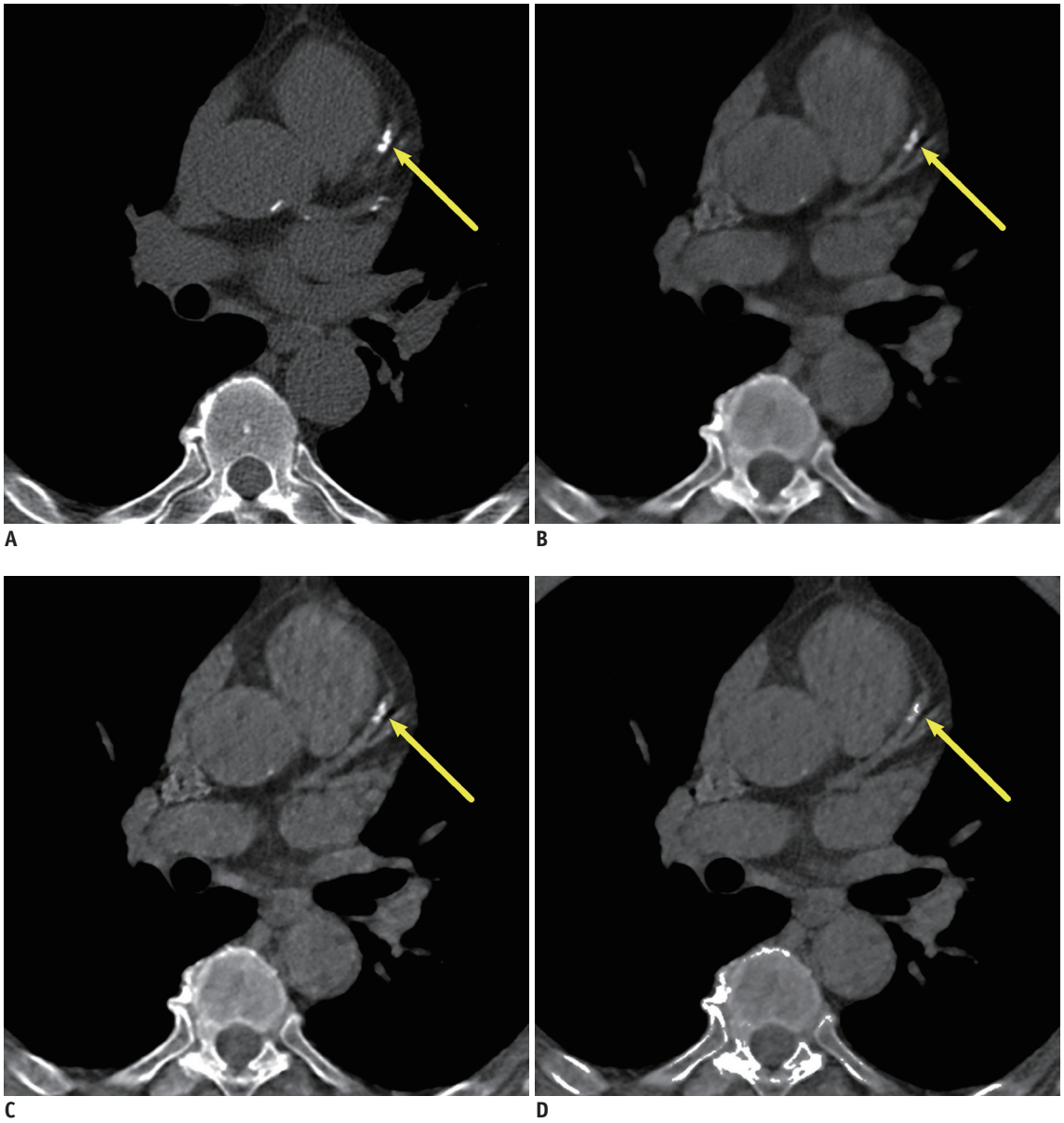

Fig. 1. Reconstructed images of corresponding axial 2.5-mm sections of heart in 70-year-old man.
A. True noncontrast-enhanced image used as reference standard shows calcification in left anterior descending coronary artery (arrow). **B.** Material density iodine-calcium pair image shows coronary plaque (arrow) having similar size as in reference image **(A)**. **C.** Material density iodine-water pair image shows coronary plaque (arrow) having similar size as in reference image **(A)**. **D.** Material suppressed iodine image also depicts clearly calcification (arrow) but looks smaller than in reference image **(A)**.

The calcium score of each lesion was calculated as described by Agatston et al. (19), by multiplying the area of each calcification by the corresponding attenuation factor derived from the maximal Hounsfield unit (HU) within the area. Pixels that had a CT value equivalent to the 130 HU threshold were calibrated based on comparison between CT values of water and soft tissue from MDW and MDC images. Determined threshold values were 1100 HU for MDW images and 900 HU for MDC images. For MSI images, 130 HU was used for threshold. The volume score was based on a calculation of the number of voxels in the volume data set that belong to the calcification, multiplied by the volume of one voxel (20). All measurements from TNC images (130 HU threshold) were used as reference standards. False-positive and false-negative calcium scores or volumes from VNC images were assessed.

Statistical Analyses

Statistical analysis was performed using dedicated statistical software (SPSS 17.0; SPSS Inc., Chicago, IL, USA). Variables were tested for normal distribution by using the Kolmogorov-Smirnov test. Nonparametric tests were used for variables that lacked a normal distribution; the Wilcoxon signed-rank test was used for paired samples. Nonparametric continuous variables were described as medians with interquartile ranges (IQR). The correlation between the calcium scores and volumes from the TNC images and those from the VNC images was expressed by a nonparametric Spearman correlation coefficient.

For the analyses, CAC scores of zero and CAC volumes of

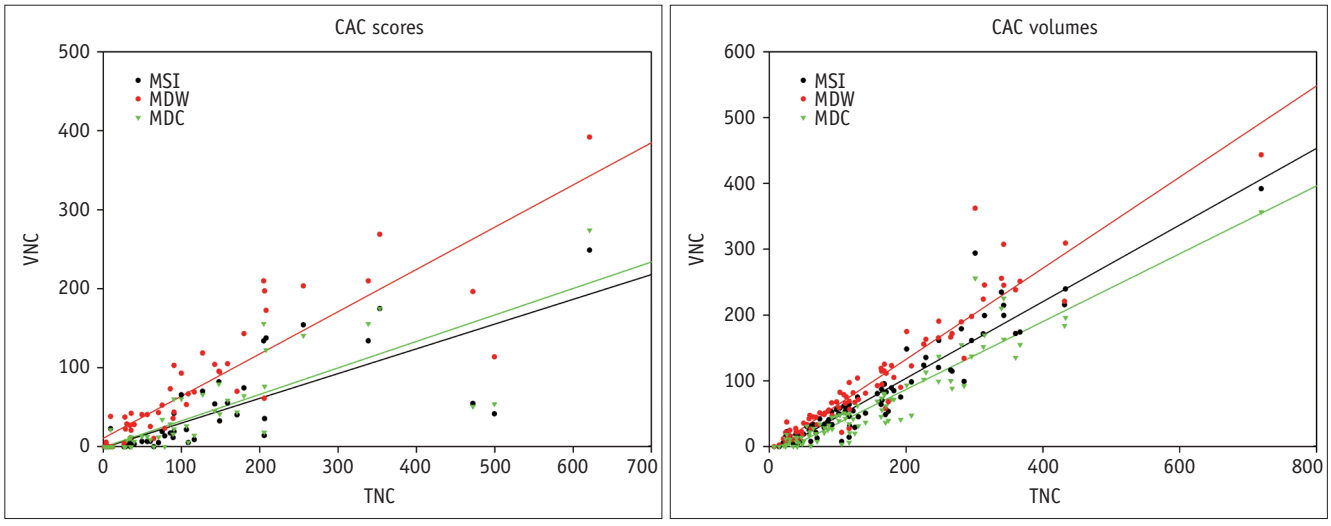

A B

Fig. 2. Scatter-plots of CAC scores (A) and volumes (B) from TNC images and VNC images.
A. Association between coronary artery calcium (CAC) scores from virtual noncontrast-enhanced (VNC) images and those from TNC images evaluated by calculation of Spearman's correlation coefficients. Scatter-plots show excellent correlation between CAC scores from VNC images and those from TNC images (Spearman's correlation coefficient [ρ] = 0.935, 0.875, and 0.890 for MDW, MDC, and MSI, respectively; $p < 0.001$ for all pairs). **B.** Association between CAC volumes from VNC images and those from TNC images. Scatter-plots show excellent correlation between CAC volumes from VNC images and those from TNC images (ρ = 0.923, 0.865, and 0.906 for MDW, MDC, and MSI, respectively; $p < 0.001$ for all pairs). MDC = material density iodine-calcium pair, MDW = material density iodine-water pair, MSI = material suppressed iodine, TNC = true noncontrast-enhanced

Table 1. Spearman's Correlation Coefficients of Virtual Noncontrast Images Compared with True Noncontrast Image for Measurement of Coronary Artery Calcium and Other Vessels

	Coronary Artery				Other Vessels			
	Calcium Score		Calcium Volume		Calcium Score		Calcium Volume	
	ρ	*P*	ρ	*P*	ρ	*P*	ρ	*P*
MDW	0.935	< 0.001	0.923	< 0.001	0.969	< 0.001	0.957	< 0.001
MDC	0.875	< 0.001	0.865	< 0.001	0.942	< 0.001	0.922	< 0.001
MSI	0.890	< 0.001	0.906	< 0.001	0.934	< 0.001	0.939	< 0.001

ρ (rho) means Spearman's correlation coefficients. MDC = material density iodine-calcium pair, MDW = material density iodine-water pair, MSI = material suppression iodine

Korean Journal of Radiology
KJR

zero were excluded because the CAC scores and volumes from the VNC images were zero in all the patients who had a CAC score of zero or CAC volume of zero from the TNC images; therefore, such a correlation in cases with a CAC score of zero or CAC volume of zero may overestimate the correlation coefficient. The CAC score and volume were compared between TNC images and VNC images using Bland-Altman analysis. A *p* value of less than 0.05 was considered statistically significant.

RESULTS

Quantified CACS from the TNC images were plotted against that from the VNC images (Fig. 2). Fifty-four of 97 patients (55.7%) had CAC scores and volumes greater than zero from the TNC images. In 54 patients, the median coronary calcium scores were 77.1 (IQR 29.1–148.6) from the TNC images, 11.1 (0.6–42.0) on MSI, 42.5 (21.1–101.0) from MDW, and 13.5 (0–53.2) from MDC images. The median calcium volumes were 58.2 (21.8–132.1) mm^3 from the TNC images, 10.7 (0.4–37.6) mm^3 from MSI, 23.9 (8.0–64.5) mm^3 from MDW, and 4.14 (0–25.7) mm^3 from MDC images. The CAC scores and volumes were significantly lower from the VNC images than from the TNC images (Wilcoxon signed-rank test, $p < 0.001$ for all pairs).

The correlation coefficients of calcium measurements for the coronary artery between VNC (three methods) and TNC (as reference standard) images are shown in Table 1. Forty-three patients (44.3%) had a CAC score of zero and also a CAC volume of zero from the TNC images. CACS from all three VNC images showed excellent correlation with those from TNC images (Spearman's correlation coefficient [ρ] = 0.935, 0.875, and 0.890 for MDW, MDC, and MSI, respectively; $p < 0.001$ for all pairs). Measured coronary calcium volumes from VNC images also correlated well with those from TNC (ρ = 0.923, 0.865, and 0.906 for MDW, MDC, and MSI, respectively; $p < 0.001$ for all pairs). Among the three VNC images, coronary calcium from MDW correlated best with that from TNC. Bland-Altman plots with limits of agreement showed a systematic error due to an underestimation of CAC scores and volumes

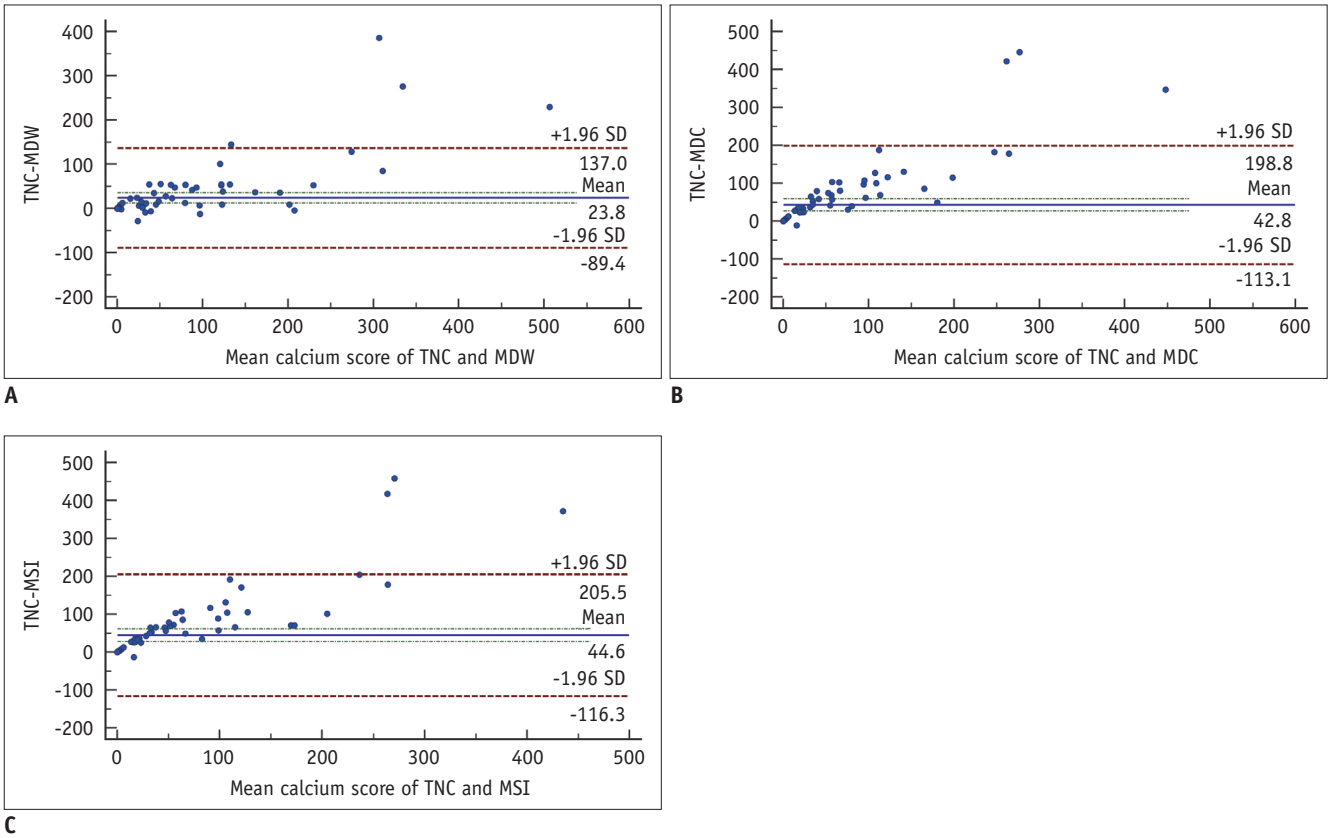

Fig. 3. Bland-Altman plots of CAC scores between TNC image and MDW (A), MDC (B), MSI (C) images.
Mean CAC score from TNC image and VNC images is plotted against difference between two methods. solid blue line = mean difference (bias) between two measurements, dashed green lines = 95% confidence intervals for that difference, dashed red lines = limits of agreement between two measurements. CAC = coronary artery calcium, MDC = material density iodine-calcium pair, MDW = material density iodine-water pair, MSI = material suppressed iodine, TNC = true noncontrast-enhanced, VNC = virtual noncontrast-enhanced

of VNC images. The mean differences between TNC and VNC images increased with higher CAC scores and volumes with the use of either method (Figs. 3, 4).

There were no false-positive calcium scores from any of the VNC images. There were 8 false-negative calcium scores (scores of 0) in MDW images and 14 among each of the MSI and MDC images.

Calcium was identified on other vessels for 83 patients (85.6%) from the TNC images. In 83 patients, the median calcium scores of other vessels were 178.7 (70.0–248.6) from the TNC images, 98.9 (22.3–121.2) from MSI, 144.2 (52.9–197.1) from MDW, and 95.4 (59.0–204.5) from MDC images. The median volumes were 145.6 (59.0–204.5) mm^3 from the TNC images, 79.4 (19.3–98.6) mm^3 from MSI, 96.2 (33.3–129.6) mm^3 from MDW, and 70.8 (14.7–84.9) mm^3 from MDC images. The calcium scores and volumes of other vessels were significantly lower from the VNC images than from the TNC images (Wilcoxon signed-rank test, $p < 0.001$ for all pairs).

Fourteen patients (14.4%) had a calcium score of zero and also a calcium volume of zero from the TNC images. Total calcium scores of other vessels from all three VNC images correlated well with those from TNC images ($\rho = 0.969$, 0.942, and 0.934 for MDW, MDC, and MSI, respectively; $p < 0.001$ for all pairs). Measured calcium volumes of other vessels from VNC images also correlated well with those from TNC images ($\rho = 0.957$, 0.922, and 0.939 for MDW, MDC, and MSI, respectively; $p < 0.001$ for all pairs). Among the three VNC images, calcium of other vessels from MDW correlated best with that from TNC.

There were 1, 2, and 4 false-negative (calcium scores of 0) calcium scores from MDW, MSI, and MDC images, respectively. There were no false-positive calcium scores in any of the VNC images.

DISCUSSION

Our prospective study shows that calcium scores and volumes of the coronary artery from VNC images derived from single-source fast kVp-switching dual-energy chest

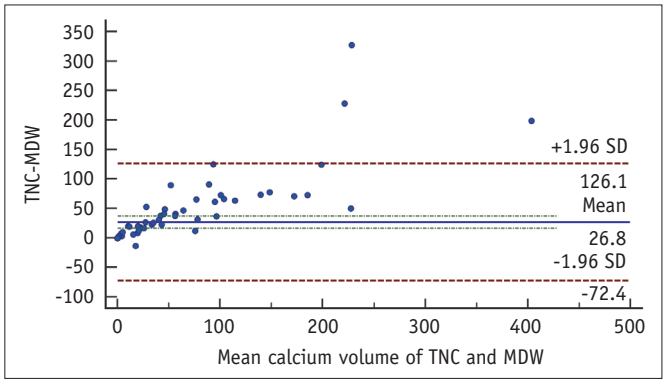

A

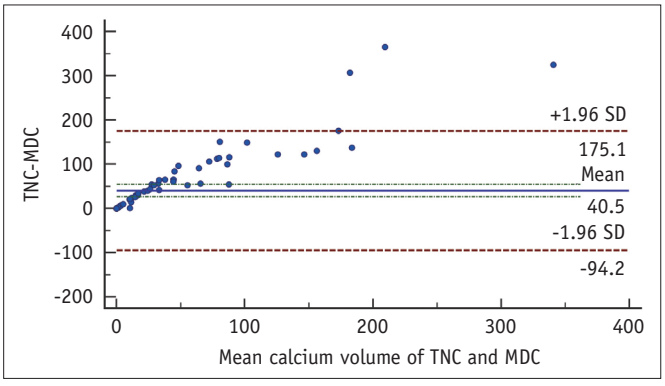

B

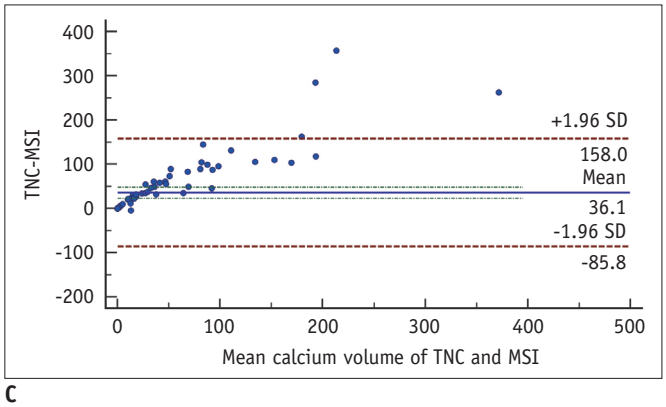

C

Fig. 4. Bland-Altman plots of CAC volumes between TNC image and MDW (A), MDC (B), MSI (C) images.
Mean CAC volume from TNC image and VNC images is plotted against difference between two methods. solid blue line = mean difference (bias) between two measurements, dashed green lines = 95% confidence intervals for that difference, dashed red lines = limits of agreement between two measurements. CAC = coronary artery calcium, MDC = material density iodine-calcium pair, MDW = material density iodine-water pair, MSI = material suppressed iodine, TNC = true noncontrast-enhanced, VNC = virtual noncontrast-enhanced

Korean Journal of Radiology
KJR

CT correlate excellently with those from TNC images. These findings suggest that VNC images could potentially replace TNC images, which are routinely used for the quantification of coronary calcium; this change would result in reduced patient exposure to radiation and reduced scanning time, by obviating the need for acquisition of TNC images. Furthermore, we found that calcium scores and volumes of other vessels (proximal neck vessels, the aortic arch, and the descending thoracic aorta) derived from VNC images also correlated excellently with those from TNC images.

Although CAC scoring is typically performed with noncontrast-enhanced ECG-gated CT examinations to minimize motion artifacts related to cardiac movement, technological advances in multidetector CT resulting in improved temporal and spatial resolution mean that visualization of atherosclerotic calcification in the coronary arteries and the thoracic aorta has become common, even when ECG-gating is not used (21, 22). Previous studies have reported high concordance between CACS derived from non-gated low-dose chest CT and CACS derived from ECG-gated cardiac CT (23-27). To the best of our knowledge, no studies demonstrating the feasibility of CAC scoring from various VNC images using non-gated single-source DECT have been published.

According to our results, all three VNC images (MDW, MDC, and MSI) derived from contrast-enhanced single-source DECT data could potentially be used for CAC scoring as well as for scoring of major thoracic vessels. Of all the VNC images, the MDW imaging protocol provided the best correlation with coronary calcium from TNC images (ρ = 0.935 for coronary calcium scores and 0.923 for volume; p < 0.001). MDW images also showed the lowest number of false-negative calcium scores and volumes. Schwarz et al. (28) have reported on the feasibility of using VNC images derived from dual-source DECT data for CAC scoring with an image-based three-material decomposition algorithm, which was different from the VNC algorithm used in this study (projection-based two-material decomposition algorithm). Yamada et al. (18) have evaluated the feasibility of CAC scoring using VNC images derived from ECG-gated fast kVp-switching dual-energy CCTA with a projection-based multi-material decomposition algorithm. In their study, they analyzed VNC images derived from the MSI algorithm and showed excellent correlation between the CAC scores from the VNC images and TNC images.

We found that the overall calcium scores and volumes of coronary arteries and other vessels were significantly lower from the VNC images than from the TNC images. The bias in the positive direction of the Bland-Altman plot indicated that VNC images generally yielded lower CAC scores and volumes than TNC images with an increase of coronary calcium burden, potentially requiring transformation or a correction factor for direct comparison with TNC images. These findings were also demonstrated in previous studies in which the image-based three-material decomposition algorithm or projection-based two-material decomposition algorithm was used (18, 28). Underestimation of calcification from VNC images may result from erroneous subtraction of calcium in postprocessing, reduction of beam hardening or blooming, and misregistration artifacts related to cardiac and respiratory movement.

In our study, the overall false-negative rates for calcium scores and volumes from the three VNC images were higher in coronary arteries than in other vessels (proximal neck vessels, the aortic arch, and the descending thoracic aorta), and the correlation coefficients for coronary arterial calcium scores and volumes from VNC images were usually lower than those for other vessels. This might be explained by cardiac motion artifacts related to ungating. Cardiac motion artifacts are known to artificially raise calcium (29). The TNC images used as reference standards in our study were obtained using an ungated protocol, and might overestimate the calcium burden of coronary arteries.

Some study limitations need to be addressed. First, scans were obtained using non-ECG-gated contrast-enhanced chest CT. In spite of several previous studies showing that CACS determined with non-ECG-gated chest CT correlated well with that derived from ECG-gated cardiac CT (23-27), non-ECG-gated CT might be less accurate than dedicated cardiac CT due to possible cardiac motion artifacts. Second, our population showed a relatively low value for coronary calcium scores and volumes as compared with previous studies (18, 28); therefore the spectrum of patients with a higher CACS might be under-represented. Third, we did not perform per-vessel analysis.

The current study represents a single center experience using 97 patients. Further study is needed with a larger population or postprocessing software that may provide reliable VNC images for CAC scoring.

In conclusion, excellent correlation was observed between the CAC scores from the VNC images and TNC images based on contrast-enhanced CT using single-source fast-kVp switching dual-energy scanning, which may obviate the need for noncontrast images. Therefore, according to

our results, the prediction of CACS based on single-source spectral chest CT seems clinically feasible and should be further evaluated.

REFERENCES

1. Polonsky TS, McClelland RL, Jorgensen NW, Bild DE, Burke GL, Guerci AD, et al. Coronary artery calcium score and risk classification for coronary heart disease prediction. *JAMA* 2010;303:1610-1616
2. Budoff MJ, Shaw LJ, Liu ST, Weinstein SR, Mosler TP, Tseng PH, et al. Long-term prognosis associated with coronary calcification: observations from a registry of 25,253 patients. *J Am Coll Cardiol* 2007;49:1860-1870
3. Greenland P, LaBree L, Azen SP, Doherty TM, Detrano RC. Coronary artery calcium score combined with Framingham score for risk prediction in asymptomatic individuals. *JAMA* 2004;291:210-215
4. Wexler L, Brundage B, Crouse J, Detrano R, Fuster V, Maddahi J, et al. Coronary artery calcification: pathophysiology, epidemiology, imaging methods, and clinical implications. A statement for health professionals from the American Heart Association. Writing Group. *Circulation* 1996;94:1175-1192
5. Greenland P, Bonow RO, Brundage BH, Budoff MJ, Eisenberg MJ, Grundy SM, et al. ACCF/AHA 2007 clinical expert consensus document on coronary artery calcium scoring by computed tomography in global cardiovascular risk assessment and in evaluation of patients with chest pain: a report of the American College of Cardiology Foundation Clinical Expert Consensus Task Force (ACCF/AHA Writing Committee to Update the 2000 Expert Consensus Document on Electron Beam Computed Tomography) developed in collaboration with the Society of Atherosclerosis Imaging and Prevention and the Society of Cardiovascular Computed Tomography. *J Am Coll Cardiol* 2007;49:378-402
6. Mylonas I, Alam M, Amily N, Small G, Chen L, Yam Y, et al. Quantifying coronary artery calcification from a contrast-enhanced cardiac computed tomography angiography study. *Eur Heart J Cardiovasc Imaging* 2014;15:210-215
7. Otton JM, Lønborg JT, Boshell D, Feneley M, Hayen A, Sammel N, et al. A method for coronary artery calcium scoring using contrast-enhanced computed tomography. *J Cardiovasc Comput Tomogr* 2012;6:37-44
8. van der Bijl N, Joemai RM, Geleijns J, Bax JJ, Schuijf JD, de Roos A, et al. Assessment of Agatston coronary artery calcium score using contrast-enhanced CT coronary angiography. *AJR Am J Roentgenol* 2010;195:1299-1305
9. Glodny B, Helmel B, Trieb T, Schenk C, Taferner B, Unterholzner V, et al. A method for calcium quantification by means of CT coronary angiography using 64-multidetector CT: very high correlation with Agatston and volume scores. *Eur Radiol* 2009;19:1661-1668
10. Coursey CA, Nelson RC, Boll DT, Paulson EK, Ho LM, Neville AM, et al. Dual-energy multidetector CT: how does it work, what can it tell us, and when can we use it in abdominopelvic imaging? *Radiographics* 2010;30:1037-1055
11. Flohr TG, McCollough CH, Bruder H, Petersilka M, Gruber K, Süss C, et al. First performance evaluation of a dual-source CT (DSCT) system. *Eur Radiol* 2006;16:256-268
12. Johnson TR, Krauss B, Sedlmair M, Grasruck M, Bruder H, Morhard D, et al. Material differentiation by dual energy CT: initial experience. *Eur Radiol* 2007;17:1510-1517
13. Graser A, Johnson TR, Hecht EM, Becker CR, Leidecker C, Staehler M, et al. Dual-energy CT in patients suspected of having renal masses: can virtual nonenhanced images replace true nonenhanced images? *Radiology* 2009;252:433-440
14. Brown CL, Hartman RP, Dzyubak OP, Takahashi N, Kawashima A, McCollough CH, et al. Dual-energy CT iodine overlay technique for characterization of renal masses as cyst or solid: a phantom feasibility study. *Eur Radiol* 2009;19:1289-1295
15. Zou Y, Silver MD. Analysis of fast kV-switching in dual energy CT using a pre-reconstruction decomposition technique. *Proc SPIE* 2008 March 18 [Epub]. http://dx.doi.org/10.1117/12.772826
16. Mendonca PR, Bhotika R, Maddah M, Thomsen B, Dutta S, Licato PE, et al. Multi-material decomposition of spectral CT images. *Proc SPIE Med Imaging: Phys Med Imaging* 2010;7622:76 221W1-76 221W9
17. Yamak D, Pavlicek W, Boltz T, Panse PM, Frakes D, Akay M. Coronary calcium quantification using contrast-enhanced dual-energy computed tomography scans. *J Appl Clin Med Phys* 2013;14:4014
18. Yamada Y, Jinzaki M, Okamura T, Yamada M, Tanami Y, Abe T, et al. Feasibility of coronary artery calcium scoring on virtual unenhanced images derived from single-source fast kVp-switching dual-energy coronary CT angiography. *J Cardiovasc Comput Tomogr* 2014;8:391-400
19. Agatston AS, Janowitz WR, Hildner FJ, Zusmer NR, Viamonte M Jr, Detrano R. Quantification of coronary artery calcium using ultrafast computed tomography. *J Am Coll Cardiol* 1990;15:827-832
20. Callister TQ, Cooil B, Raya SP, Lippolis NJ, Russo DJ, Raggi P. Coronary artery disease: improved reproducibility of calcium scoring with an electron-beam CT volumetric method. *Radiology* 1998;208:807-814
21. Shemesh J, Henschke CI, Shaham D, Yip R, Farooqi AO, Cham MD, et al. Ordinal scoring of coronary artery calcifications on low-dose CT scans of the chest is predictive of death from cardiovascular disease. *Radiology* 2010;257:541-548
22. Jacobs PC, Gondrie MJ, Mali WP, Oen AL, Prokop M, Grobbee DE, et al. Unrequested information from routine diagnostic chest CT predicts future cardiovascular events. *Eur Radiol* 2011;21:1577-1585
23. Budoff MJ, Nasir K, Kinney GL, Hokanson JE, Barr RG, Steiner R, et al. Coronary artery and thoracic calcium on noncontrast thoracic CT scans: comparison of ungated and gated examinations in patients from the COPD Gene cohort. *J Cardiovasc Comput Tomogr* 2011;5:113-118
24. Jacobs PC, Isgum I, Gondrie MJ, Mali WP, van Ginneken

B, Prokop M, et al. Coronary artery calcification scoring in low-dose ungated CT screening for lung cancer: interscan agreement. *AJR Am J Roentgenol* 2010;194:1244-1249
25. Einstein AJ, Johnson LL, Bokhari S, Son J, Thompson RC, Bateman TM, et al. Agreement of visual estimation of coronary artery calcium from low-dose CT attenuation correction scans in hybrid PET/CT and SPECT/CT with standard Agatston score. *J Am Coll Cardiol* 2010;56:1914-1921
26. Wu MT, Yang P, Huang YL, Chen JS, Chuo CC, Yeh C, et al. Coronary arterial calcification on low-dose ungated MDCT for lung cancer screening: concordance study with dedicated cardiac CT. *AJR Am J Roentgenol* 2008;190:923-928
27. Kim SM, Chung MJ, Lee KS, Choe YH, Yi CA, Choe BK. Coronary calcium screening using low-dose lung cancer screening: effectiveness of MDCT with retrospective reconstruction. *AJR Am J Roentgenol* 2008;190:917-922
28. Schwarz F, Nance JW Jr, Ruzsics B, Bastarrika G, Sterzik A, Schoepf UJ. Quantification of coronary artery calcium on the basis of dual-energy coronary CT angiography. *Radiology* 2012;264:700-707
29. Brown SJ, Hayball MP, Coulden RA. Impact of motion artefact on the measurement of coronary calcium score. *Br J Radiol* 2000;73:956-962